

University of Jon Doe

Thesis

Title of the thesis

If you want you can have a subtitle

Jon Doe

October 9, 2025

Prof. Dr. rer. LaTeX

Contents

List of Figures

List of Tables

List of Listings

1 | Introduction

Lithium ion batteries (LIBs) have become the backbone of modern portable electronics and electric vehicles.^{Goodenough2013} When Sony commercialized the first LIB in 1991,^{VanNoorden2014} it marked the beginning of a transformation in energy storage that would eventually earn Whittingham, Goodenough, and Yoshino the 2019 Nobel Prize in Chemistry.^{Goodenough2013} The advantages of LIBs over earlier rechargeable systems (higher energy and power densities, higher operating voltages, and longer cycle life)^{VanNoorden2014} have made them the dominant technology in today's applications.

The basic operating principle of a LIB involves two intercalation electrodes (anode and cathode) separated by a lithium-ion conducting electrolyte and porous separator. During discharge, Li^+ ions leave the graphite anode and travel through the electrolyte to the cathode (typically a lithium metal oxide), while electrons flow through the external circuit; charging reverses this process. Graphite has emerged as the standard anode material because it accommodates Li^+ ions between its graphene layers (forming LiC_6) with relatively little structural change. However, the low potential of lithiated graphite lies outside the electrochemical stability window of most organic electrolytes, which leads to electrolyte decomposition and formation of a solid electrolyte interphase (SEI) on the anode surface. This nanoscale passivation layer blocks electron transport while allowing Li^+ ions to pass through, though its initial formation irreversibly consumes some lithium. Despite this cost, the SEI prevents ongoing electrolyte breakdown and is critical for long-term battery stability.^{Goodenough2013}

Battery performance, internal resistance, and lifetime all depend heavily on these interfacial processes (SEI formation, charge-transfer kinetics, and ionic transport through the electrolyte). Increasing interfacial resistance or persistent side reactions (such as electrolyte decomposition or electrode degradation) gradually reduce battery capacity by consuming active lithium and raising internal resistance.^{Goodenough2013}

A range of electrochemical characterization techniques exist to probe these interfacial processes. Cyclic voltammetry (CV) measures current as a function of swept voltage, revealing redox reactions and their reversibility. A reversible redox process produces symmetric oxidation and reduction peaks whose separation and shape reflect Nernstian equilibrium and diffusion effects, while kinetic limitations cause peak shifts and distortion.^{Elgrishi2018}

Galvanostatic charge-discharge testing (cycling at constant current) remains the standard technique for evaluating battery capacity, energy efficiency, and rate capability. These measurements yield specific capacity (mAh g^{-1}) and Coulombic efficiency (the discharge-to-charge capacity ratio) for each cycle.

Electrochemical impedance spectroscopy (EIS) takes a different approach by applying small AC perturbations across a range of frequencies. This technique excels at separating different

1 Introduction

interfacial processes by fitting the measured impedance to equivalent circuit models. The high-frequency intercept in a Nyquist plot typically corresponds to electrolyte resistance, while mid- to low-frequency features (semicircles or Warburg slopes) reflect double-layer capacitance, charge-transfer resistance, and diffusion impedance. Fitting these spectra extracts quantitative parameters like charge-transfer resistance, exchange current, and diffusion coefficients. Unlike large-perturbation methods, EIS operates near equilibrium, which allows precise characterization of both fast and slow processes. **Lazanas2023**

Together, voltammetric, galvanostatic, and impedance techniques provide complementary insights into electrochemical interfaces, identifying thermodynamic, kinetic, and transport properties.

2 | Experimental Section

3 Results

3.1 Coin-cell cycling (Task 3.1)

We did not perform cyclic voltammetry (CV) on the assembled coin cells; therefore, this section focuses on galvanostatic charge–discharge characterization at 0.1 C, 1 C, and 2 C, together with incremental capacity (dQ/dE) analysis and voltage–time transients.

3.1.1 Potential–capacity profiles

?? overlays the specific capacity *vs.* potential curves at the three C–rates. At the low rate (0.1 C), the discharge capacity is highest and the (de)lithiation plateaus are most clearly developed. With increasing rate (1 C and 2 C), polarization grows (larger charge–discharge hysteresis) and the accessible capacity decreases, consistent with kinetic and transport limitations. The chosen voltage window (2.4 V to 4.2 V) spans the practical operating region of the NCM 811 | graphite full cell; at low rate it enables utilization of most of the available capacity, while at higher rates kinetic limitations dominate the accessible capacity.

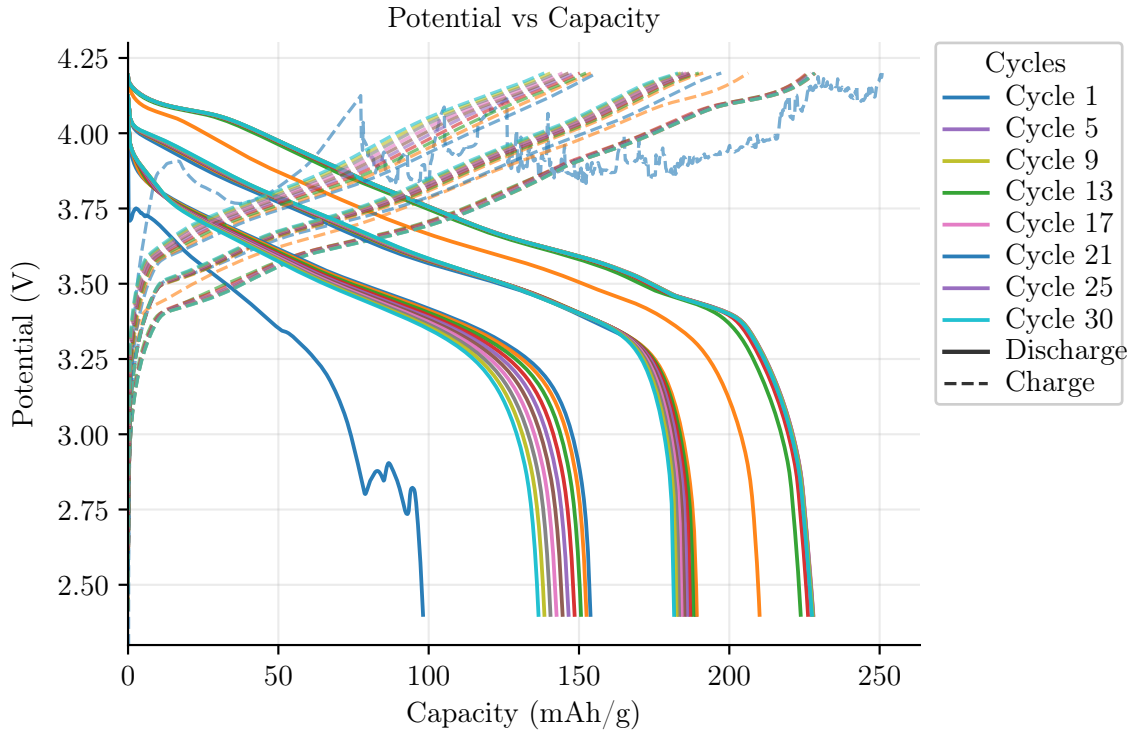


Figure 1: Potential *vs.* specific capacity at 0.1 C, 1 C and 2 C for the assembled coin cell. Higher C–rates exhibit increased polarization and reduced accessible capacity compared to 0.1 C.

3.1.2 Incremental capacity (dQ/dE) analysis

The incremental capacity plots in ?? highlight potential-resolved processes during charge and discharge. Distinct features observed at 0.1 C broaden and diminish in amplitude at 1 C and 2 C, reflecting increased overpotentials and reduced time available for phase transitions. Only cathodic processes are considered when assigning discharge features. The overall trend—peak shifting to higher/lower potentials with rate and decreasing peak area—is consistent with transport and kinetic limitations at higher C-rates.

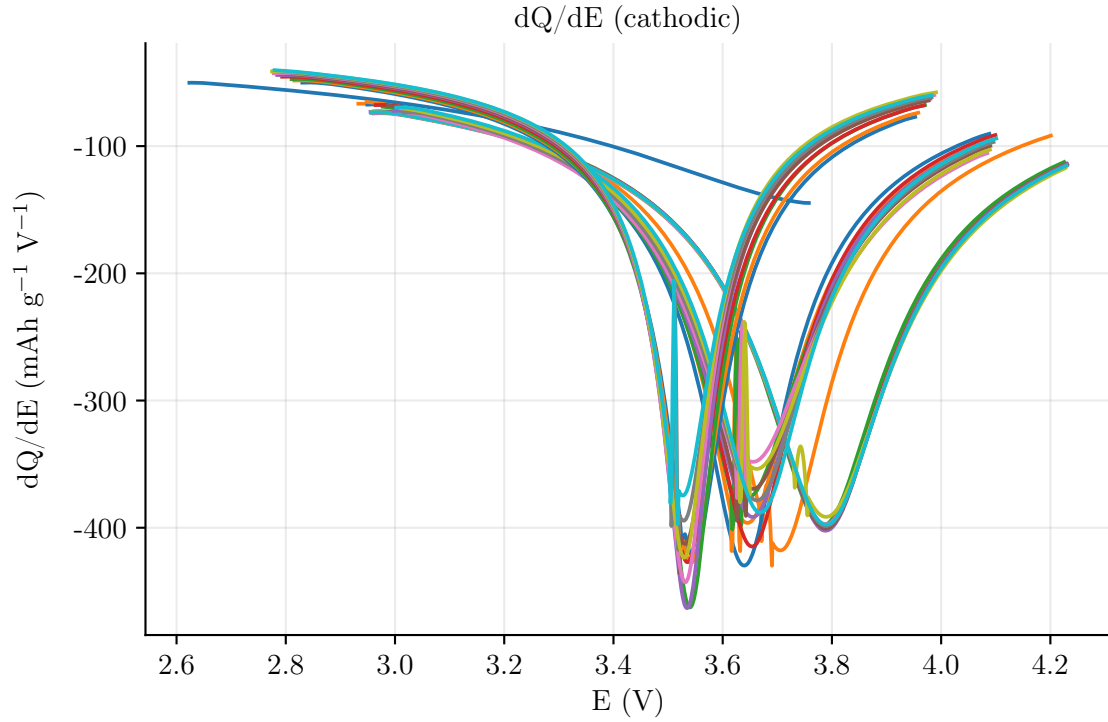


Figure 2: Incremental capacity (dQ/dE) *vs.* potential for cycling at 0.1 C, 1 C and 2 C. Increasing rate broadens and depresses features, consistent with higher polarization and reduced time for phase transitions.

3.1.3 Voltage–time transients

?? shows the voltage *vs.* time profiles at the three rates. As expected, the total charge/discharge time scales inversely with C-rate (longest at 0.1 C, shortest at 2 C). The more pronounced flat regions at low rate correlate with the sharper dQ/dE features, while at higher rate the profiles are more sloped due to increased IR drop and kinetic losses.

Figure 3: Voltage *vs.* time at 0.1 C, 1 C and 2 C. Faster rates shorten the (dis)charge durations and increase overall polarization.

3.1.4 Coulombic efficiency

The Coulombic efficiency (CE) was evaluated as the ratio of discharge to charge capacity for each cycle. At 0.1 C, CE rapidly approaches near-unity after initial formation, indicating minimal parasitic reactions once the SEI is stabilized. At higher rates (1 C and 2 C), CE remains high but can show a slightly larger deviation from unity, consistent with increased polarization and potential side reactions at elevated current. Across all three rates, the trends are consistent with a well-behaved NCM811|graphite full cell operating within the selected voltage window.

4 | Conclusion